Chemical Engineering Journal 434 (2022) 134708

Contents lists available at ScienceDirect

Chemical Engineering Journal

journal homepage: www.elsevier.com/locate/cej

Short communication

Insights on uranium removal by ion exchange columns: The deactivation mechanisms, and an overlooked biological pathway

Fan Chen [a,1], Miao Lv [b,1], Yin Ye [a,*], Shiyu Miao [c], Xin Tang [a], Yang Liu [c], Bin Liang [d], Zemin Qin [a], Yanlong Chen [a], Zhangwei He [e], Yuheng Wang [a,*]

[a] School of Ecology and Environment, Northwestern Polytechnical University, Xi'an 710129, PR China
[b] Faculty of Geosciences and Environmental Engineering, Southwest Jiaotong University, Chengdu 611756, PR China
[c] College of Eco-Environmental Engineering, Qinghai University, Xining 810016, PR China
[d] State Key Laboratory of Urban Water Resource and Environment, School of Civil and Environmental Engineering, Harbin Institute of Technology Shenzhen, Shenzhen 518055, PR China
[e] School of Environmental and Municipal Engineering, Xi'an University of Architecture and Technology, Xi'an 710055, PR China

ARTICLE INFO

Keywords:
Uranium removal
Ion exchange
Functional bacteria
Microbial interaction
Seepage water treatment

ABSTRACT

Ion exchange (IX) is an attractive approach to extract uranium from wastewater, simultaneously reducing the negative environmental impact of uranium mining and recovering uranium resources. However, the IX process is limited by the deactivation of the resin, and the role played by microorganisms attached to the resin remains unknown. Here, we characterized the chemical and mineralogical compositions, microbial community structure, and network-related molecular mechanism of the uranium-bearing deposit on SBA exchange resin from a full-scale U mine seepage water treatment system. The uranium removal by the resin was attributed to the formation of binary anionic $UO_2(SO_4)_2^{2-}$ or $UO_2(SO_4)_3^{4-}$ complexes and their subsequent association with the resin. The deactivation of the resins might mainly result from the presence of deposits on the resin surface rather than the saturation of functional groups. Microbial reduction of U(VI) to U(IV) was confirmed in the deposit. The long-term operation acclimated functional microbial communities on the resin, such as *Curvibacter* sp., *Acidovorax* sp., and *Herminiimonas* sp. for uranium bioremediation, *Methylotenera* sp. for biofilm formation, and *Polaromonas* sp. and *Hydrogenophaga* sp. for autotrophic metabolism. Molecular ecological network analysis indicated the synthetic metabolisms among metal remediation bacteria and autotrophs might play major roles in microbial-mediated uranium removal. This study offers new insights into the application of the IX system for uranium-containing wastewater treatment.

1. Introduction

Nuclear power and its primary fuel, uranium (U), play a crucial in decarbonizing the global energy supply [1,2]. Along with the flourish of the nuclear power industry, large quantities of U-containing wastewater are released during the mining and milling of U ores [3]. As U is highly hazardous to the biosphere, the wastewater can pose serious threats to the ecosystem if not properly treated [4].

Uranyl ($U^{VI}O_2^{2+}$) is the dominant U species in U-containing wastewater [5]. Ion exchange (IX) is the most adopted technique for the removal of U(VI) in wastewater treatment practices [6,7]. Strong base anion (SBA) exchange resins possess quaternary amine groups ([-N$(CH_3)_3$OH]), a wide operating pH range and high selectivity for U. SBA are hence the most commonly used IX resins in the treatment of U-containing wastewater [5]. To date, much research efforts in U removal by IX have focused on novel material development, removal efficiency and capacity, and operating conditions for certain treatment objectives [7–10]. However, in industrial operations, the progressive deactivation of IX resins remains constantly a bottleneck of this widely implemented technology [11]. Historically, the IX-based U mine wastewater treatment process is generally-perceived as a pure physical–chemical water treatment process. The blockage of IX functional groups by extracted ions is generally considered to be the main reason for the resin deactivation [12]. However, the IX efficiency depends on both the mass

* Corresponding authors.
E-mail addresses: yeyin01@hotmail.com (Y. Ye), yuheng.wang@nwpu.edu.cn (Y. Wang).
[1] Fan Chen and Miao Lv contributed equally to this work.

https://doi.org/10.1016/j.cej.2022.134708
Received 6 November 2021; Received in revised form 20 December 2021; Accepted 11 January 2022
Available online 17 January 2022
1385-8947/© 2022 Elsevier B.V. All rights reserved.

transfer processes and the ion adsorption/exchange process [13], especially the former [14]. Therefore, the obstructed mass transfer might be also responsible for the resin deactivation in the IX process.

During the long-term continuous operation of IX columns, the resins provide a suitable environment for microorganism attachment and growth thanks to their macroporous structure [15]. Meanwhile, the resin matrix material can be used as nutrients for microorganism growth [16,17]. Therefore, the formation of biofilms on the resin surfaces is inevitable in IX systems [16], which may result in biofouling and lower mass transfer efficiency, even reduced lifetime and higher operational costs. Moreover, the presence of biofilms allows for the potential long-term microbial U metabolism [18]. Processes involving microorganisms, such as bioreduction, bioaccumulation, biosorption and bioprecipitation, could immobilize U [19]. Therefore, an in-depth understanding of the microbial-mediated activities in IX columns will be helpful for the implementation of IX techniques. However, the information of microorganisms attached to the resin under real-world settings is scarce, and whether and how the microbial community in resin biofilm impacts U removal remain unknown.

Therefore, we aim to reveal the underneath deactivation mechanisms of IX resins in a full-scale IX column treating real U mine seepage water. The objectives of this study are to (1) decipher the mechanisms of IX resin deactivation; (2) confirm the microbial-mediated U removal in the IX system; (3) identify the core members and microbial interactions in the resin biofilm. This study offers new insights on the deactivation mechanisms of IX resins in treating U-containing waste streams, which may facilitate future practical implementations of IX systems in U-containing wastewater treatment.

2. Materials and methods

2.1. Materials

The resins were taken from a full-scale fixed-bed IX column for treating the tailings seepage water of a U mine located in western China. The resins were a strong basic anion exchange type (201 × 7, gel-type) characterized by the quaternary amine functional group ([-N$(CH_3)_3$OH]), with a nominal saturation capacity of 6.5 mg/mLR. The treatment process of the seepage water is shown in Fig. S1. The average U concentration in the treated wastewater was about 5 mg/L, and the influent pH fluctuated between 6.2 and 6.8. The wastewater was oligotrophic with an organic carbon content of less than 10 mg/L. Six fixed resin beds were divided into two groups, with three in series in each group. The height of each resin bed was 4 m, and the speed of the empty adsorption bed was 15 m/h. Six saturated resin samples (S1-S6) were collected from six resin beds after a continuous operation of six months. The regenerated resin (S0) was collected after rinsing with $NaHCO_3$/NaCl solutions. The fresh resin before adsorption was also collected for a blank control.

2.2. Characterizations

The resins used for the following characterization were dried under a continuously purified nitrogen atmosphere in a glove box (Unilab, Mbraun). Scanning electron microscopy (SEM) and energy dispersive spectroscopy (EDS) were conducted using a JSM-7900F (JEOL) ultra-high-resolution FE-SEM equipped with an X-Max N EDS system. The resins were coated with an ultrathin coating of platinum (Pt) by low-vacuum sputter before SEM characterization, and the coated Pt was subtracted to accurately express element composition. X-ray photoelectron spectroscopy (XPS) was carried out using a Thermo K-Alpha + XPS with an Al (Kα) source. Fourier Transform Infrared Spectroscopy (FT-IR) was measured in the range of 4000–400 cm^{-1} on a Perkin-Elmer Spectrum One FT-IR spectrometer (Perkin-Elmer, USA).

2.3. Microbial community analysis

To collect biomass from resin surface, the resin first washed with sterile water under rigorous oscillation. Subsequently, the resin was removed and the remaining liquid mixture was centrifuged at 12000 rpm for 15 min, and the precipitates collected were the biomass. The details for DNA extraction, PCR amplification, Illumina MiSeq sequencing and taxonomic classification have been described in previous studies [20–22]. The microbial community structure and molecular ecological network analysis were performed using the Majorbio Cloud Platform (www.majorbio.com). The Spearman correlations between the top 30 abundances of bacteria were calculated for the network construction [23]. The raw sequencing data of 16S rRNA genes were deposited in the NCBI database (Accession number: PRJNA752976).

3. Results and discussion

3.1. The uranium removal and resin deactivation mechanisms

The IX system studied herein could reduce the U in the seepage water from ~ 5 mg/L to less than 0.3 mg/L. After a long-term operation, the actual breakthrough volume was only 40% of the nominal saturation volume (1000 BV vs. 2500 BV). When U concentration in the resin reached 500 mg/L, the rinsing process would be performed to reduce U concentration in the resin to less than 100 mg/L. When the U concentration in the effluent was still higher than 0.3 mg/L after rinsing, the resin would be regenerated. The saturation capacity of the resin would be decreased by 5–10% after each regeneration cycle.

3.1.1. Characterization of functional groups on the resin

The FT-IR was used to investigate the structural changes in the SBA resins (Fig. 1). The broad and strong peak at 3419.06 cm^{-1} could be attributed to the stretching vibration of the hydroxyl group in the [-N$(CH_3)_3$OH] structure [8]. The characteristic peaks at 1482.86 cm^{-1} and 1619.06 cm^{-1} could be ascribed to the vibration absorption of the benzene skeleton, and the peaks at 1000–500 cm^{-1} belonged to the C–H vibration in the benzene ring [24]. The peak at 2088.63 cm^{-1} could be assigned to the stretching vibration of C-O [25], which might be attributed to the contamination of the resin by carbon-containing substances (e.g., carbon oxides, bicarbonates, natural organic matters, etc.). There was no obvious difference in these characteristic peaks among the fresh resin, the saturated resin, and the regenerated resin, except a high-intensity peak at 1114.88 cm^{-1} (S = O bond in sulfate) in the saturated resin spectrum [26], which could probably be assigned to the adsorption of SO_4^{2-} from the seepage water. This suggested that the seepage water treatment and the rinsing regeneration did not significantly alter the functional groups of the resin. Therefore, the deactivation of the resins might not result from the saturation of the active sites.

3.1.2. Morphological changes of the resin surface

To examine whether the mass transfer was suppressed, the resin morphologies were characterized using SEM (Fig. S2). The results showed that the resins were spherically shaped, and the fresh resin exhibited smooth morphology while the saturated resin was covered by crust-like deposits. Compared with saturated resin, the deposits on the surface of regenerated resin were noticeably reduced but still observable.

The elemental composition analysis results showed that the resin was enriched in Fe, S, U, Si and Al (17.33%, 4.84%, 2.79%, 2.69% and 2.01% (wt%), respectively) (Fig. 2). Especially, the elemental mapping confirmed that the U and S were rather homogeneously distributed on the entire resin surface, whereas Fe, Si and Al were concentrated in the crust-like deposits, which occupied most of the resin surface. The U mine where the IX resin was collected employs a sulfuric acid-based leaching approach to solubilize the U from ores, leading to a high concentration of SO_4^{2-} (650 ± 50 mg/L) in the seepage water. In the seepage water, U

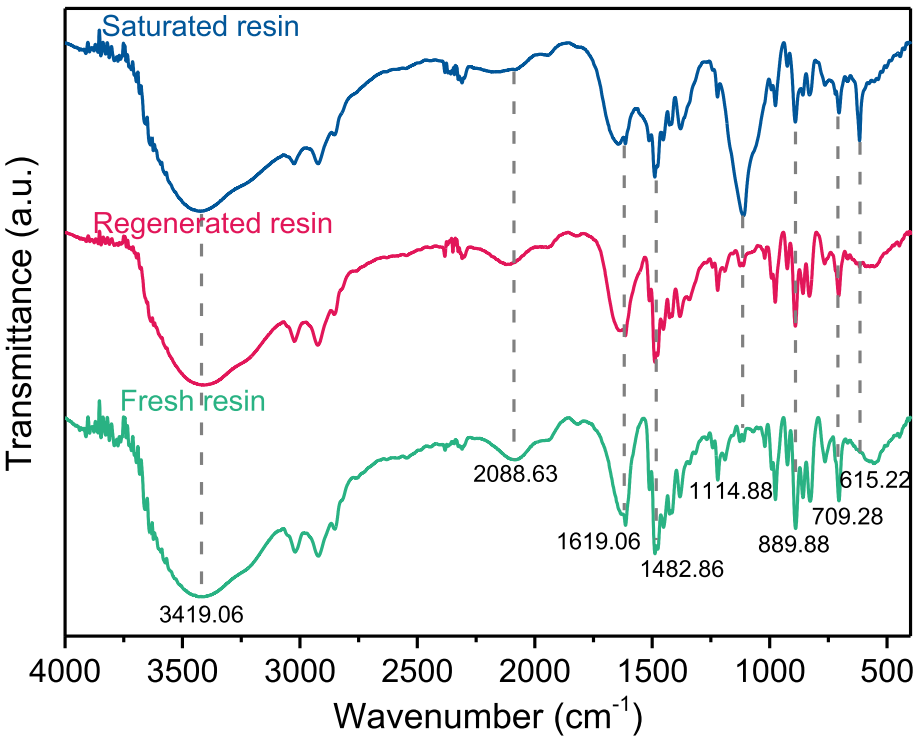


Fig. 1. FT-IR spectra of the fresh resin, saturated resin and regenerated resin.

exists in the form of uranyl structures. Theoretically, this aqueous uranyl would complex with co-existing anions to form UO_2^{2+}-anion complexes, especially under neutral or basic conditions (Eqs (1)–(2)) [6,27].With increasing anion-to-uranyl ratio, the proportion of UO_2^{2+}-anion complexes increases [5]. Considering the near-neutral pH (6.2–6.8), with a high sulfate-to-uranyl ratio in the seepage water, it is logical to conclude that the predominant U species was UO_2^{2+}-SO_4^{2-} complexes [6,27]. Previous studies also reported that the efficient U uptake by the SBA exchange resins was attributed to the adsorption of anionic $UO_2(SO_4)_2^{2-}$ or $UO_2(SO_4)_3^{4-}$ complexes [5,6], which confirmed the correlation between the distribution of U and S. The reactions involved in the sorption of $UO_2(SO_4)_2^{2-}$ or $UO_2(SO_4)_3^{4-}$ by SBA exchange resins were shown in Eqs. (3)–(4).

$$UO_2^{2+} + 2SO_4^{2-} \rightleftharpoons UO_2(SO_4)_2^{2-} \quad (1)$$

$$UO_2^{2+} + 3SO_4^{2-} \rightleftharpoons UO_2(SO_4)_3^{4-} \quad (2)$$

$$2ROH + UO_2(SO_4)_2^{2-} \rightarrow R_2UO_2(SO_4)_2 + 2OH^- \quad (3)$$

$$4ROH + UO_2(SO_4)_3^{4-} \rightarrow R_4UO_2(SO_4)_3 + 4OH^- \quad (4)$$

Besides, a fraction of U was adsorbed on the crust-like deposits. These deposits could increase the resistance to mass transfer across the boundary layer surrounding the resin particles and reduce intra-particle diffusion [13]. On the other hand, no change of the functional group ([-N(CH_3)$_3$OH]) of the resin was observed using FT-IR spectroscopy (Fig. 1). Therefore, the decrease of adsorption capacity could mainly be attributed to the deposits covering the resin surface, rather than the failure of functional groups.

3.2. Reduction of uranium in the IX column

To further elucidate the U removal mechanisms, the saturated resin was characterized using XPS (Fig. 3). Two characteristic U4f peaks emerged, indicating the U deposition on the resin, which was consistent with the SEM-EDS results (Fig. 2). The U4f scan spectrum showed two major peaks separated from each other by ~ 10.9 eV due to the spin–orbit split (Fig. 3a). The two U4f peaks could be assigned to the $U4f_{7/2}$ and $U4f_{5/2}$, respectively. The U4f binding energies of both peaks were ~ 1.0 eV lower than that of uranyl nitrate (Fig. 3b), indicating that the surface deposited U in the saturated resin was at least partly reduced [28]. Further, the U4f scan spectrum was fit to investigate the valence state of the deposited U [29]. As U(VI) is the dominant and the most stable uranium redox state in the seepage water, the XPS evidence of U (IV) indicated the reduction of deposited U(VI) in the IX resins column (Fig. 3a).

In theory, U(VI) reduction can take place via biological, chemical, and photochemical processes [30]. In anoxic systems, sulfide (S^{2-}), hydrogen (H_2), Fe(II), and zerovalent iron (Fe^0) can reduce U(VI) [31,32]. In this study, the mine seepage water to be treated by the IX column was stored in the open air, hence the chemical reduction of U (VI) should be negligible [30]. In addition, the IX column was made of opaque materials, which ruled out light irradiation and the possibility of photochemical U(VI) reduction. On the other hand, as the formation of biofilms is inevitable in the long-term continuous operation of IX columns treating non-sterilized wastewaters [15,16], and a variety of environmentally relevant bacteria exhibit U(VI) reductive capacity [32], the U(VI) reduction here is inferred to be the result of microbial metabolic activity.

3.3. Potential functional bacterial genera in resin biofilm

Detailed information on sequencing information, diversity, dominating phyla and classes were illustrated in supplementary data (Fig. S3). At the genus level, *Curvibacter* (11.9%-42.4%), *Acidovorax* (4.47%-17.5%), *Methylotenera* (2.0%-29.8%), *Hydrogenophaga* (2.0%-20.8%), *Polaromonas* (1.0%-5.2%), *Herminiimonas* (0.4%-12.8%), *Pseudomonas* (1.4%-3.9%) and *Massilia* (0.4%-8.6%) dominated the resin biofilms. Although the types of the bacterial genera enriched on the surface of regenerated and saturated resins shared high similarities, their relative abundances still showed an obvious difference (Fig. 4 and S4).

Most of the dominant bacteria have the function of metal

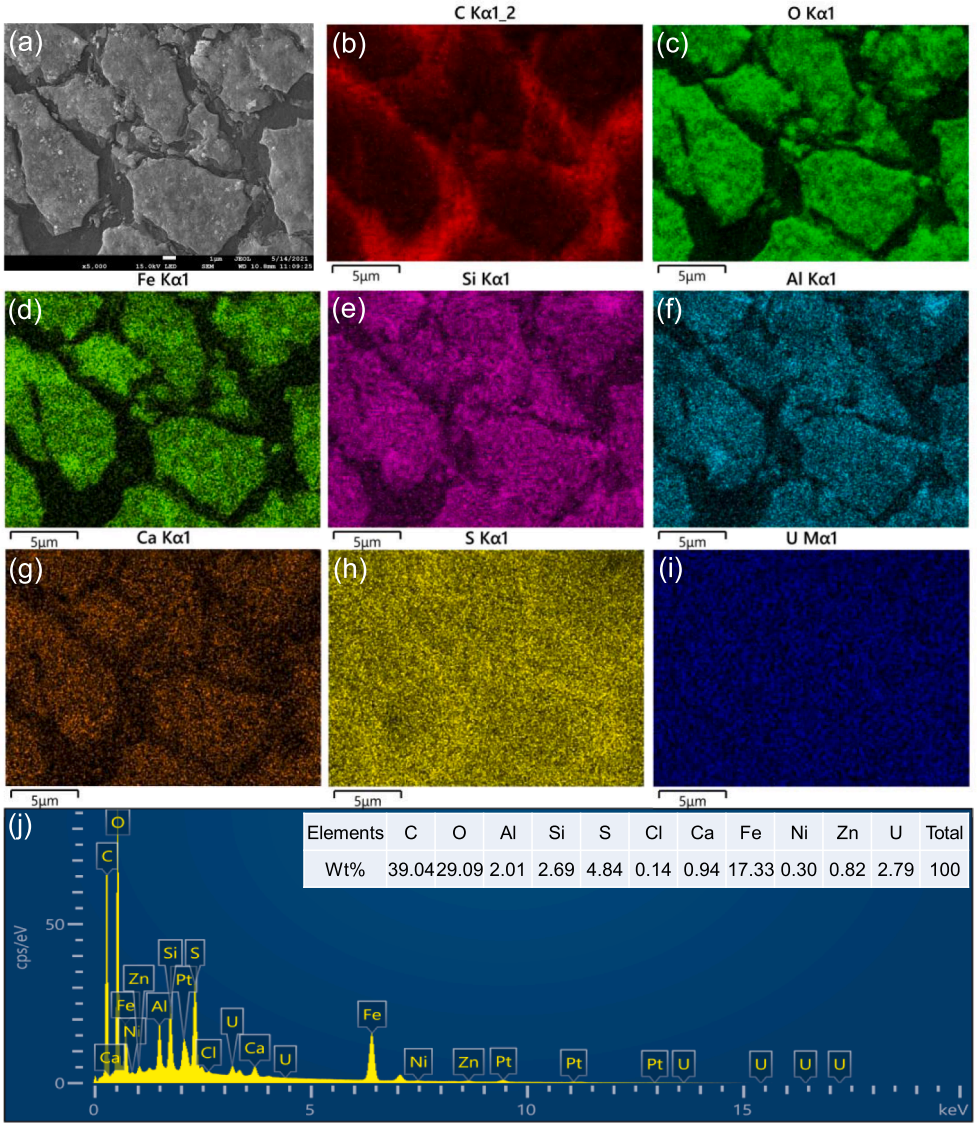


Fig. 2. (a) SEM image, (b-i) elemental mappings, and (j) EDS spectrum of the saturated SBA resin.

bioremediation. Specifically, *Curvibacter* sp. can resist and bioremediate U at a concentration of 2 mM [33]. *Acidovorax facilis* was a suitable candidate for *in situ* U bioremediation through biosorption on the cell surface and intracellular accumulation [34]. *Herminiimonas* was reported to be metal resistant and present in an acid mine drainage microbial community [35,36]. *Sediminibacterium* sp. was able to tolerate U and was previously recovered from metal-rich sediment [37]. Oligotrophic *Limnobacter* bacteria was also observed in the community within uranium ore [38]. *Pseudomonas* strains could tolerate and bioremediate heavy metals and metalloids, including U, iron, etc. [39]. Previous studies have confirmed the multiple-metal (e.g., Zn^{2+} and Ni^{2+}) resistance of *Massilia* sp. [40]. Also, some low-abundance metal-reducing bacteria, such as *Ferribacterium* (less than1.8%) and *Geobacter* (less than1.7%) with the ability to reduce U(VI) to U(IV), were observed in the saturated resins [41,42]. This finding is consistent with the observed U(VI) reduction (Fig. 3).

In addition, functional communities involved in biofilm formation and autotrophic metabolism were found to be abundant (Fig. 4). *Methylotenera* is one widely known biofilm-forming organism, which could secrete a high amount of extracellular polymeric substances [43]. Hence it may play an important role in the formation of biofilm on resin. Besides, *Methylotenera* was reported to be highly enriched in the soils or groundwater with high metal contents [44]. *Polaromonas* and *Hydrogenophaga* were observed in freshwater environments and dominated in the biofilm of the filters treating ultraoligotrophic water [45]. In oligotrophic solutions, the microbial growth is enhanced when they can settle on a resin surface, attributed to the nutrient accumulation on the surface by adsorption. Therefore, the long-term operation acclimated the collaborative functional communities on the resin, such as *Curvibacter* sp., *Acidovorax* sp., and *Herminiimonas* sp. for metal bioremediation, *Methylotenera* sp. for biofilm formation, and *Polaromonas* sp. and *Hydrogenophaga* sp. for autotrophic metabolism.

3.4. Molecular ecological network of the potential core bacterial genera

The Venn diagram showed bacterial community structures of the resin biofilms displayed noticeable overlap with each other (Fig. 5a). The majority shared OTUs were affiliated with the putative functional genera such as *Curvibacter* (OTU697: 25.81%), *Acidovorax* (OTU226: 11.53%), *Methylotenera* (OTU699: 11.15%), *Hydrogenophaga* (OTU63: 10.16%), *Herminiimonas* (OTU146: 6.94%), unclassified_f_*Comamonadaceae* (OTU675: 4.88%), *Sediminibacterium* (OTU535: 4.23%), *Limnobacter* (OTU647: 3.43%), *Massilia* (OTU471: 2.26%) (Fig. 5b).

We applied a molecular ecological network approach to explore the

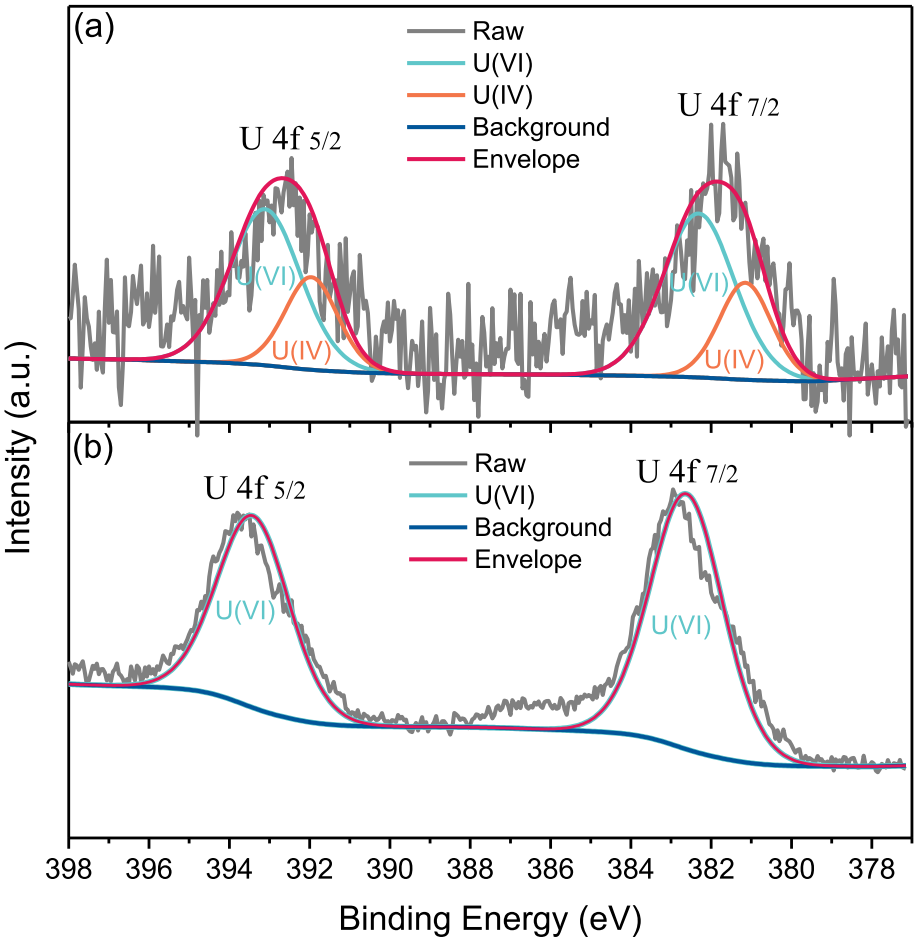


Fig. 3. XPS U 4f scan of (a) the saturated resin and (b) uranyl nitrate.

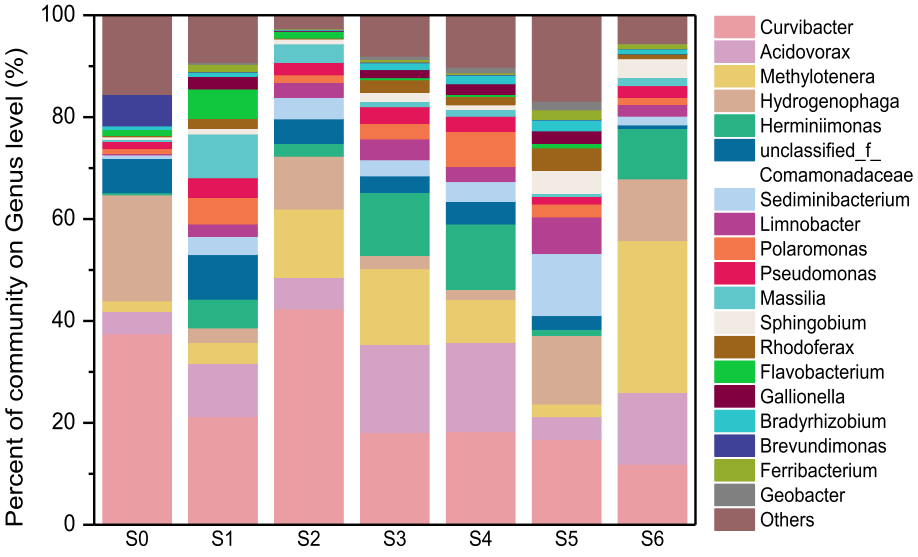


Fig. 4. Bacterial community structures of the resin biofilm at genera level. S0: the biofilm of the regenerated resin; S1-S6: the biofilms of saturated resins collected from six different adsorption beds.

interaction between different species. The overall network for the 30 most abundant genera was divided into three distinct modules based on their relationships (Fig. 6). In the first module, the node of OTU697 categorized as *Curvibacter* showed 13 links (interactions) with other OTUs, and 84.6% of the interactions were negative. Especially, both *Acidovorax* (OTU226) and *Herminiimonas* (OTU146) showed a negative correlation with *Curvibacter* (OTU697), representing their potential competing relationships. While *Curvibacter* (OTU697), *Hydrogenophaga* (OTU63) and *Sediminibacterium* (OTU535) were positively correlated with each other, all of them were negatively correlated with other OTUs,

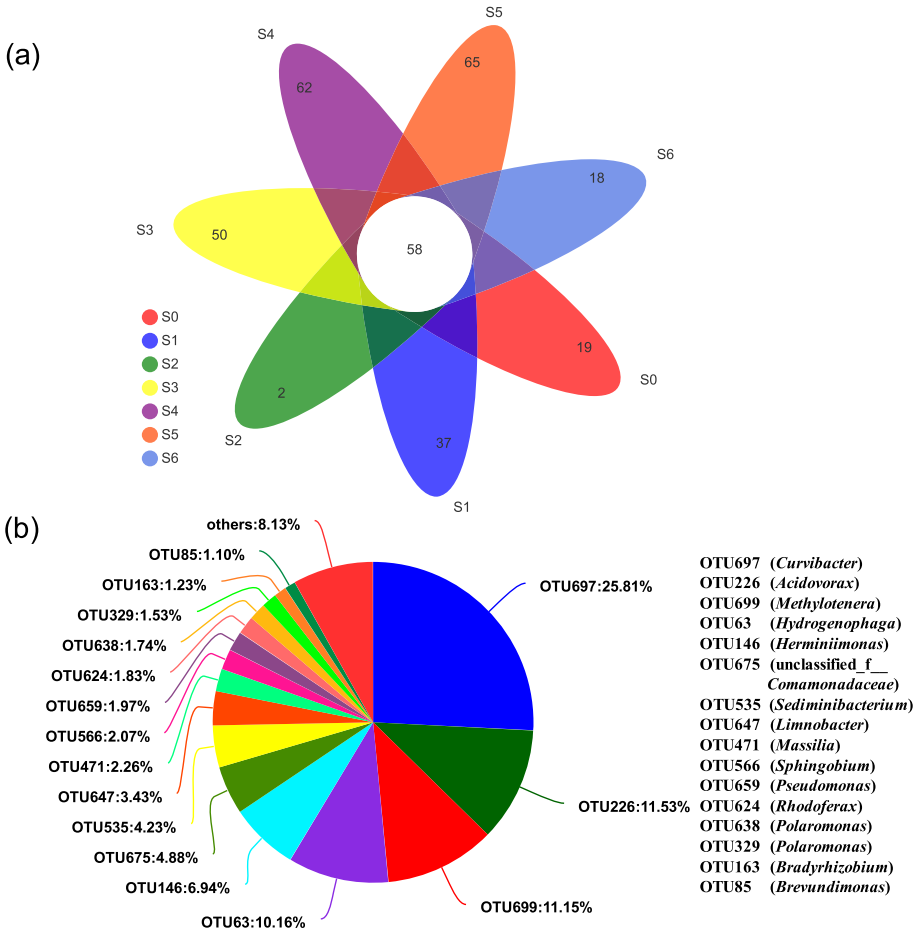


Fig. 5. (a) Venn diagram of OTUs among each of resin biofilms and (b) the composition of the sharing OTUs.

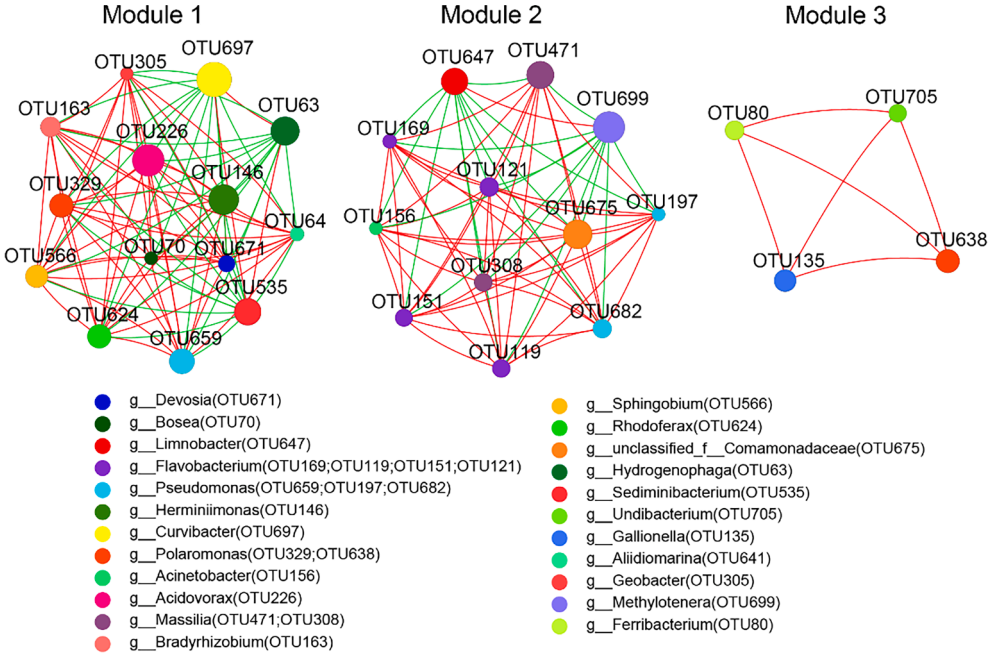


Fig. 6. Network diagram of species correlation in resin biofilms (nodes with different colors represent different species; node size represents species abundance; the red line represents positive correlation, and the green line indicates negative correlation).

indicating their tight cooperative activities or similar preferred ecological niche. It was worth noting that *Acidovorax* (OTU226) and *Herminiimonas* (OTU146) were positively correlated. In the second module, *Methylotenera* (OTU699) displayed a positive correlation with *Limnobacter* (OTU647), while both of them were negatively correlated with other OTUs, implying the similar phylogenetic relatedness between them. Interestingly, the two dominant genera, unclassified_f_*Comamonadaceae* (OTU675) and *Massilia* (OTU471) had a positive correlation with other OTUs except for *Methylotenera* (OTU699) and *Limnobacter* (OTU647).

Based on the above mutual relationships, we could separate the dominant bacteria into five groups (group 1, group 2, group 3, group 4 and group 5). *Curvibacter* (OTU697), *Hydrogenophaga* (OTU63) and *Sediminibacterium* (OTU535) were in group 1; *Acidovorax* (OTU226), *Herminiimonas* (OTU146), *Polaromonas* (OTU329) and *Geobacter* (OTU305) in group 2; *Methylotenera* (OTU699) and *Limnobacter* (OTU647) in group 3; unclassified_f_*Comamonadaceae* (OTU675), *Massilia* (OTU471; OTU308) and *Flavobacterium* (OTU169; OTU119; OTU151; OTU121) in group 4; *Ferribacterium* (OTU80), *Polaromonas* (OTU638), *Gallionella* (OTU135) and *undibacterium* (OTU705) in group 5, respectively. All of the internal links within each group were positive, whereas the intergroup links were composed of negative interactions or no obvious correlation. It was clear that the metal remediation bacteria took important positions in the network of each group and the core metal-reducing bacteria of each group were different. More importantly, the interactions between metal remediation bacteria and autotrophic bacteria (e.g., *Curvibacter* and *Hydrogenophaga* in group 1; *Acidovorax* and *Polaromonas* in group 2*; Ferribacterium* and *Polaromonas* in group 5) were positive, which implied the strong affinity of metal remediation bacteria with the autotrophic bacteria. In the oligotrophic U-mine seepage water, autotrophs might utilize inorganic bicarbonate as the carbon source to synthesize organic compounds, contributing to the thriving of heterotrophic metal reduction bacteria. Therefore, the synthetic metabolisms among metal reduction bacteria and autotrophs might form the foundation of the reduction mechanism for the dissolved U. In addition, the interactions between members may buffer the whole community function against environmental perturbation [46].

In the future, an in-depth understanding of the microbiomes in the resin surface is necessary to answer how microbial interactions drive U (VI) reduction. Further, determining a complete metabolic flux of microbial communities is meaningful for decoding the microbial-mediated U removal pathways in the full-scale IX system, which is a valuable though challenging research direction for the future. As our results indicated, the formation of scarcely soluble U(IV) is detrimental to the mass transfer, so removal of the U(IV)-containing deposits on the resin surface is the key to avoiding progressive deactivation of resins, possible approaches include dosing of oxidants or air-purging.

4. Conclusions

The U removal was attributed to the formation of binary anionic $UO_2(SO_4)_2^{2-}$ or $UO_2(SO_4)_3^{4-}$ complexes and their subsequent association with the resin. The deactivation of the resins might mainly result from the presence of deposits on the resin surface rather than the saturation of functional groups. Microbial reduction of U(VI) to U(IV) was confirmed in the deposit. The long-term continuous operation acclimated functional microbial communities on the resin with the functions of uranium bioremediation, biofilm formation, and autotrophic metabolism. The synthetic metabolisms among metal reduction bacteria and autotrophs might form the foundation of U(VI) reduction mechanism.

Declaration of Competing Interest

The authors declare that they have no known competing financial interests or personal relationships that could have appeared to influence the work reported in this paper.

Acknowledgements

This research was supported by the fellowship of China Postdoctoral Science Foundation (2021M692637), the National Natural Science Foundation of China (No. 42077352), and the Qinghai Science and Technology Department Project (No. 2018-ZJ-703).

Appendix A. Supplementary data

Supplementary data to this article can be found online at https://doi.org/10.1016/j.cej.2022.134708.

References

[1] R. Rhodes, More nuclear power can speed CO_2 cuts, Nature 548 (2017) 281-281.
[2] C. Degueldre, Uranium as a renewable for nuclear energy, Prog. Nucl. Energy 94 (2017) 174–186.
[3] D.H. Dang, W. Wang, P. Pelletier, A.J. Poulain, R.D. Evans, Uranium dispersion from U tailings and mechanisms leading to U accumulation in sediments: Insights from biogeochemical and isotopic approaches, Sci. Total Environ. 610–611 (2018) 880–891.
[4] N. Gao, Z. Huang, H. Liu, J. Hou, X. Liu, Advances on the toxicity of uranium to different organisms, Chemosphere 237 (2019), 124548.
[5] J.T.M. Amphlett, M.D. Ogden, R.I. Foster, N. Syna, K. Soldenhoff, C.A. Sharrad, Polyamine functionalised ion exchange resins: synthesis, characterisation and uranyl uptake, Chem. Eng. J. 334 (2018) 1361–1370.
[6] J.T.M. Amphlett, S. Choi, S.A. Parry, E.M. Moon, C.A. Sharrad, M.D. Ogden, Insights on uranium uptake mechanisms by ion exchange resins with chelating functionalities: chelation vs. anion exchange, Chem. Eng. J. 392 (2020), 123712.
[7] Z. Wen, K. Huang, Y. Niu, Y. Yao, S. Wang, Z. Cao, H. Zhong, Kinetic study of ultrasonic-assisted uranium adsorption by anion exchange resin, Colloids Surf., A 585 (2020) 124021, https://doi.org/10.1016/j.colsurfa.2019.124021.
[8] L. Chen, Y. Chen, X. Wang, Y. Wei, L. He, F. Tang, A novel silica-based anion exchange resin used for removing uranium from drinking water, J. Radioanal. Nucl. Chem. 314 (3) (2017) 2569–2578.
[9] D. Ma, J. Wei, Y. Zhao, Y. Chen, S. Tang, The removal of uranium using novel temperature sensitive urea-formaldehyde resin: adsorption and fast regeneration, Sci. Total Environ. 735 (2020) 139399, https://doi.org/10.1016/j.scitotenv.2020.139399.
[10] S. Wen, Y.e. Sun, R. Liu, L. Chen, J. Wang, S. Peng, C. Ma, Y. Yuan, W. Gong, N. Wang, Supramolecularly poly (amidoxime)-loaded macroporous resin for fast uranium recovery from seawater and uranium-containing wastewater, ACS Appl. Mater. Interfaces 13 (2) (2021) 3246–3258.
[11] J.-C. Lee, Kurniawan, H.-J. Hong, K.W. Chung, S. Kim, Separation of platinum, palladium and rhodium from aqueous solutions using ion exchange resin: A review, Sep. Purif. Technol. 246 (2020) 116896, https://doi.org/10.1016/j.seppur.2020.116896.
[12] I. Levchuk, J.J. Rueda Márquez, M. Sillanpää, Removal of natural organic matter (NOM) from water by ion exchange-A review, Chemosphere 192 (2018) 90–104.
[13] J. Zhang, A. Amini, J.A. O'Neal, T.H. Boyer, Q. Zhang, Development and validation of a novel modeling framework integrating ion exchange and resin regeneration for water treatment, Water Res. 84 (2015) 255–265.
[14] M. Zhang, A. Li, Q. Zhou, C. Shuang, W. Zhou, M. Wang, Effect of pore size distribution on tetracycline adsorption using magnetic hypercrosslinked resins, Microporous Mesoporous Mater. 184 (2014) 105–111.
[15] J. Winter, H.E. Wray, M. Schulz, R. Vortisch, B. Barbeau, P.R. Bérubé, The impact of loading approach and biological activity on NOM removal by ion exchange resins, Water Res. 134 (2018) 301–310.
[16] H.-C. Flemming, Biofouling and me: my stockholm syndrome with biofilms, Water Res. 173 (2020), 115576.
[17] H.-C. Flemming, Microbial growth on ion exchangers, Water Res. 21 (7) (1987) 745–756.
[18] C. Zhou, A. Ontiveros-Valencia, L. Cornette de Saint Cyr, A.S. Zevin, S.E. Carey, R. Krajmalnik-Brown, B.E. Rittmann, Uranium removal and microbial community in a H_2-based membrane biofilm reactor, Water Res. 64 (2014) 255–264.
[19] Y.V. Nancharaiah, S.V. Mohan, P.N.L. Lens, Biological and bioelectrochemical recovery of critical and scarce metals, Trends Biotechnol. 34 (2) (2016) 137–155.
[20] F. Chen, Z.-L. Li, M. Lv, C. Huang, B. Liang, Y. Yuan, X.-Q. Lin, X.-Y. Gao, A.-J. Wang, Recirculation ratio regulates denitrifying sulfide removal and elemental sulfur recovery by altering sludge characteristics and microbial community composition in an EGSB reactor, Environ. Res. 181 (2020), 108905.
[21] Z.-W. He, C.-X. Yang, C.-C. Tang, W.-Z. Liu, A.-J. Zhou, Y.-X. Ren, A.-J. Wang, Response of anaerobic digestion of waste activated sludge to residual ferric ions, Bioresour. Technol. 322 (2021), 124536.
[22] A. Wang, K.e. Shi, D. Ning, H. Cheng, H. Wang, W. Liu, S. Gao, Z. Li, J. Han, B. Liang, J. Zhou, Electrical selection for planktonic sludge microbial community function and assembly, Water Res. 206 (2021) 117744, https://doi.org/10.1016/j.watres.2021.117744.
[23] Z.-L. Li, R. Cheng, F. Chen, X.-Q. Lin, X.-J. Yao, B. Liang, C. Huang, K. Sun, A.-J. Wang, Selective stress of antibiotics on microbial denitrification: Inhibitory effects, dynamics of microbial community structure and function, J. Hazard. Mater. 405 (2021), 124366.

[24] X. Zhu, W. Li, C. Zhang, Extraction and removal of vanadium by adsorption with resin 201* 7 from vanadium waste liquid, Environ. Res. 180 (2020), 108865.
[25] Y. Wang, F.-L. Hu, Y. Mi, C. Yan, S. Zhao, Single-metal-atom catalysts: An emerging platform for electrocatalytic oxygen reduction, Chem. Eng. J. 406 (2021), 127135.
[26] E. Salehi, M. Shafie, Adsorptive removal of acetaldehyde from water using strong anionic resins pretreated with bisulfite: An efficient method for spent process water recycling in petrochemical industry, J. Water Process Eng. 33 (2020), 101025.
[27] T. Vercouter, P. Vitorge, B. Amekraz, C. Moulin, Stoichiometries and thermodynamic stabilities for aqueous sulfate complexes of U(VI), Inorg. Chem. 47 (6) (2008) 2180–2189.
[28] Y. Wang, T. Wu, J. Barbaud, W. Kong, D. Cui, H. Chen, X. Yang, L. Han, Stabilizing heterostructures of soft perovskite semiconductors, Science 365 (2019) 687.
[29] M. Schindler, F.C. Hawthorne, M.S. Freund, P.C. Burns, XPS spectra of uranyl minerals and synthetic uranyl compounds. I: The U4f spectrum, Geochim. Cosmochim. Acta 73 (9) (2009) 2471–2487.
[30] H. Zhang, W. Liu, A. Li, D. Zhang, X. Li, F. Zhai, L. Chen, L. Chen, Y. Wang, S. Wang, Three mechanisms in one material: uranium capture by a polyoxometalate-organic framework through combined complexation, chemical reduction, and photocatalytic reduction, Angew. Chem. Int. Ed. 58 (2019) 16110–16114.
[31] S. Yan, B. Hua, Z. Bao, J. Yang, C. Liu, B. Deng, Uranium(VI) removal by nanoscale zerovalent iron in anoxic batch systems, Environ. Sci. Technol. 44 (20) (2010) 7783–7789.
[32] J.D. Wall, L.R. Krumholz, Uranium reduction, Annu. Rev. Microbiol. 60 (1) (2006) 149–166.
[33] M. Agarwal, R.S. Rathore, A. Black, X. Xu, J. Seaman, A. Chauhan, I.L.G. Newton, Announcing the availability of a culture collection of uranium-resistant microbial assemblages (CURMA) obtained from metalliferous soils of the savannah river site, USA, Microbiology Resource Announcements 9 (30) (2020), https://doi.org/10.1128/MRA.00551-20.
[34] U. Gerber, I. Zirnstein, E. Krawczyk-Bärsch, H. Lünsdorf, T. Arnold, M.L. Merroun, Combined use of flow cytometry and microscopy to study the interactions between the gram-negative betaproteobacterium *Acidovorax facilis* and uranium(VI), J. Hazard. Mater. 317 (2016) 127–134.
[35] R.R. Auld, N.C.S. Mykytczuk, L.G. Leduc, T.J.S. Merritt, Seasonal variation in an acid mine drainage microbial community, Can. J. Microbiol. 63 (2) (2017) 137–152.
[36] D. Muller, D.D. Simeonova, P. Riegel, S. Mangenot, S. Koechler, D. Lièvremont, P. N. Bertin, M.-C. Lett, *Herminiimonas arsenicoxydans* sp. nov., a metalloresistant bacterium, Int. J. Syst. Evol. Microbiol. 56 (2006) 1765–1769.
[37] M.P. Reis, F.A.R. Barbosa, E. Chartone-Souza, A.M.A. Nascimento, The prokaryotic community of a historically mining-impacted tropical stream sediment is as diverse as that from a pristine stream sediment, Extremophiles 17 (2) (2013) 301–309.
[38] E. Islam, P. Sar, Culture-dependent and -independent molecular analysis of the bacterial community within uranium ore, J. Basic Microbiol. 51 (4) (2011) 372–384.
[39] S. Choudhary, P. Sar, Uranium biomineralization by a metal resistant *Pseudomonas aeruginosa* strain isolated from contaminated mine waste, J. Hazard. Mater. 186 (1) (2011) 336–343.
[40] G.-D. Feng, S.-Z. Yang, H.-P. Li, H.-H. Zhu, *Massilia putida* sp. nov., a dimethyl disulfide-producing bacterium isolated from wolfram mine tailing, Int. J. Syst. Evol. Microbiol. 66 (2016) 50–55.
[41] U.K. Banala, N.P.I. Das, S.R. Toleti, Microbial interactions with uranium: towards an effective bioremediation approach, Environ. Technol. Innovation 21 (2021), 101254.
[42] Y. Wang, A. Bagnoud, E. Suvorova, E. McGivney, L. Chesaux, V. Phrommavanh, M. Descostes, R. Bernier-Latmani, Geochemical control on uranium(IV) mobility in a mining-impacted wetland, Environ. Sci. Technol. 48 (17) (2014) 10062–10070.
[43] B. Braun, J. Schröder, H. Knecht, U. Szewzyk, Unraveling the microbial community of a cold groundwater catchment system, Water Res. 107 (2016) 113–126.
[44] Y. Wang, P. Li, Z. Jiang, A. Sinkkonen, S. Wang, J. Tu, D. Wei, H. Dong, Y. Wang, Microbial community of high arsenic groundwater in agricultural irrigation area of hetao plain, Inner Mongolia, Front. Microbiol. 7 (2016).
[45] A. Magic-Knezev, B. Wullings, D. Van der Kooij, *Polaromonas* and *Hydrogenophaga* species are the predominant bacteria cultured from granular activated carbon filters in water treatment, J. Appl. Microbiol. 107 (5) (2009) 1457–1467.
[46] M. Qi, B. Liang, L. Zhang, X. Ma, L. Yan, W. Dong, D. Kong, L. Zhang, H. Zhu, S.-H. Gao, J. Jiang, S.-J. Liu, P.-X. Corvini, A. Wang, Microbial interactions drive the complete catabolism of the antibiotic sulfamethoxazole in activated sludge microbiomes, Environ. Sci. Technol. 55 (5) (2021) 3270–3282.